To Appear in the Astrophysical Journal

Discovery of a Dusty Ring in the Coalsack: A Dense Core Caught in the Act of Formation?

Charles J. Lada, and Tracy L. Huard

Harvard-Smithsonian Center for Astrophysics, 60 Garden Street, Cambridge MA 02138

clada@cfa.harvard.edu thuard@cfa.harvard.edu

Lionel J. Crews

Department of Geology, Geography, and Physics, University of Tennessee at Martin, Martin, TN 38238

lcrews@utm.edu

and

João F. Alves

European Southern Observatory, Garching Germany

jalves@eso.org

ABSTRACT

We present a new infrared extinction study of Globule 2, the most opaque molecular cloud core in the Coalsack complex. Using deep near-infrared imaging observations obtained with the ESO NTT we are able to examine the structure of the globule in significantly greater detail than previously possible. We find the most prominent structural feature of this globule to be a strong central ring of dust column density which was not evident in lower resolution studies of this cloud. This ring represents a region of high density and pressure that is likely a transient structure. For a spherical cloud geometry the ring would correspond to a dense inner shell of high pressure that could not be in dynamical equilibrium with its surroundings since there appear to be no sources of pressure in the central regions of the cloud that could support the shell against gravity and prevent its inward implosion. The timescale for the inward collapse of the ring

would be less than 2 x 10^5 years, suggesting that this globule is in an extremely early stage of evolution, and perhaps caught in the process of forming a centrally condensed dense core or Bok globule. Outside its central regions the globule displays a well-behaved density profile whose shape is very similar to that of a stable Bonnor-Ebert sphere. Using SEST we also obtained a $C^{18}O$ spectrum toward the center of the cloud. The CO observation indicates that the globule is a gravitationally bound object. Analysis of the CO line profile reveals significant non-thermal gas motions likely due to turbulence. As a whole the globule may be evolving to a global state of quasi-static dynamical equilibrium in which thermal and turbulent pressure balance gravity.

Subject headings: molecular clouds–dark nebulae–ISM: dust, extinction and globules

1. Introduction

Low mass dense cores found within molecular cloud complexes and isolated dark globules (also known as Bok globules) are the simplest configurations of dense molecular gas and dust known to form stars (e.g, Benson & Myers 1989; Yun & Clemens 1990). They have been long recognized as important laboratories for investigating the physical processes which lead to the formation of stars and planets (e.g., Bok 1948). In recent years deep infrared imaging surveys of such globules have provided an important new tool for detailed examination of their structure. For example, infrared observations of the starless globule B 68 produced an exquisitely detailed measurement of the cloud's radial density distribution (Alves, Lada & Lada 2001, hereafter ALL01). This density distribution was shown to match very closely that predicted for a marginally stable, pressure bounded, isothermal sphere in hydrostatic equilibrium (i.e., a Bonnor-Ebert sphere). Similar deep near-infrared observations of the darker globule B 335 enabled a detailed investigation of the radial density profile of a globule containing a central protostar. The profile in this star forming globule was found to be significantly steeper than that of B 68, consistent with expectations for a collapsed or collapsing core (Harvey et al. 2001). These observations suggest that the evolution of dense cores to form stars can be effectively traced and measured by detailed observations of the cloud's density structure, best obtained by infrared extinction observations.

Two of the least understood aspects of the star formation process are the initial conditions that describe dense cores that ultimately form stars and the origin of such dense cores from more diffuse atomic and molecular material. Deep infrared and millimeter-wave observations of starless cores or globules offer the best opportunity to investigate these issues.

Starless cores account for about 70% of optically selected dark cores and globules (Lee & Myers 1999). A particularly interesting group of cores in this regard are those associated with the conspicuous Coalsack dark cloud complex in the southern Milky Way (Tapia 1973; Bok, Sim & Hawarden 1977; Bok 1977). The entire Coalsack complex subtends an angle of roughly 6^o on the sky corresponding to a linear dimension of nearly 15 pc at the distance of 150 pc estimated for this cloud (e.g., Cambresy 1999, and references therein). A survey of ^{12}CO emission found the cloud to be characterized by complex, filamentary structure and to be relatively massive containing about 3500 $M_\odot$ of material (Nyman, Bronfman & Thaddeus 1989). However, a survey of emission from the rarer ^{13}CO isotopic line found the ratio of ^{13}CO to ^{12}CO emitting gas in the cloud to be considerably lower (17%) than that (50-80%) which characterizes nearby star forming molecular clouds (Kato et al. 1999). This observation indicated that the fraction of dense gas in the Coalsack complex is considerably smaller than that which characterizes typical star forming cloud complexes. The paucity of dense gas coupled with the lack of the usual signposts of star formation activity, such as emission-line stars, HH objects, embedded infrared sources, etc. (e.g., Kato et al. 1999) suggests that the Coalsack may be a molecular cloud complex in the earliest stages of evolution. The globules within the Coalsack are apparently all starless and also may be in the early phases of development.

Knowledge of the detailed structure of globules in the Coalsack may provide further insight concerning their physical nature and evolutionary status. In particular, it would be interesting to know to what extent the structure of a Coalsack globule resembles that of a starless cloud like B 68 or a star forming globule such as B 335. Tapia's Globule 2 is the most prominent and likely densest globule in the Coalsack (Bok et al. 1977; Kato et al. 1999). Located slightly below ($\sim 1^o$) the galactic plane, it is projected against a rich star field and is a prime candidate for infrared extinction studies. Jones et al. (1980) obtained JHK photometry of 75 stars located behind the Coalsack cloud and derived individual extinctions to all these stars. Their observations suggested a radial column density distribution that was not highly centrally concentrated. Racca, Gomez and Kenyon (2002) obtained JHK infrared images of the globule that were more sensitive and resulted in the detection of a few thousand stars behind the cloud. They used H-band star counts to construct a low resolution extinction map of the globule and derived an azimuthally averaged radial density profile which confirmed the shallow nature of the radial column density distribution. Moreover, they found that the radial density distribution could be fit by a Bonnor-Ebert configuration with a density profile quite similar to that of B 68 and considerably shallower than that of B 335.

In this paper we report new and deeper near-infrared imaging observations of Globule 2 (hereafter G2). We use these observations to determine the individual line-of-sight extinc-

tions to thousands of stars behind the cloud. These measurements enable an examination of the structure of the globule to be made in a degree of detail considerably greater than that obtained by previous studies and comparable to that acheived earlier for B 68. The high angular resolution achieved by our observations reveal the globule to be more structured than suspected previously. Moreover, these observations indicate that the spatial distribution of column density in this globule differs significantly from that of other well studied examples, such as B 68 and B 335. In particular, the radial dust column density profile of G2 is not only found to be shallow, but also to be characterized by a significant central depression that, in turn, is surrounded by a prominent ring of high column density. These characteristics suggest that Globule 2 may represent a very early stage in the evolution of cloudy material to form a centrally condensed dense core.

2. Telescopes and Instrumentation

We used the ESO 3.5-m New Technology Telescope (NTT) at the European Southern Observatory (ESO) in La Silla, Chile on 8-9 March 1999, 13 March 2000 and 18 June 2003 to obtain the imaging observations reported here. The telescope was outfitted with the infrared imager/spectrometer SOFI (Moorwood et al. 1998). SOFI is equipped with a 1024 × 1024 pixel Rockwell array which was configured to provide a field of view $\sim 5 \times 5$ arc min with a spatial resolution of 0.292 ± 0.001 arc sec pixel^{-1}. Observations were obtained with J (1.25 μm), H (1.65 μm), and K_s (2.16 μm) filters.

We also used the 15-m Swedish ESO Submillimeter Telescope (SEST) at La Silla on 28 May 2000 to obtain an observation of the $C^{18}O$ (J = 2–1) line at 219 GHz toward the center of the globule. The receiver was equipped with an SIS mixer which produced a system temperature of approximately 200 K. The half-power beamwidth at the observing frequency was approximately 24 arc sec. An AOS spectrometer provided a velocity resolution of 0.06 km sec^{-1}. A series of five minute, frequency-switched observations were summed to achieve a total integration time of 60 minutes. This resulted in an rms noise level of about 0.02 K. The calibration was done using the standard chopper wheel method which compared sky emission to an ambient temperature load to set the temperature scale for the spectra.

3. Observations, Results and Analysis

Figure 1 shows an optical image of the region around Globule 2 in the Coalsack. In order to fully image the globule, we obtained a 3 × 3 mosaic of J, H and K_s images covering

a field approximately 14 × 14 arc min approximately centered on the globule. The surveyed region is indicated by the box in Figure 1. The total effective exposure times were 50, 30, and 20 seconds for the J, H and K_s bands respectively, except in the central 5 × 5 arc min region where we observed for 95 seconds at J. Each integration consisted of a series of coadded short dithered observations. The dithers were randomly generated within a box 40 × 40 arc sec in size centered on each field in the mosaic. The data reduction was accomplished with a combination of standard Image Reduction and Analysis Facility (IRAF)[1] routines and custom software. Sources were identified and automatically extracted from the images using the SExtractor program. All images were inspected to find and extract any additional stars that were not automatically identified. Aperture photometry for all sources was obtained using standard *daophot* packages in IRAF, while their positions were derived by comparison with known positions of stars, as listed in the USNO-A2.0 catalog, that were observed in our fields. Instrumental magnitudes obtained from 2.3 arc sec diameter synthetic apertures centered on these sources, were calibrated using the J, H and K magnitudes of stars within our fields that were listed in the 2MASS catalog. Only stars having 2MASS H-K colors between 0 and 0.3 magnitudes were used for calibration to avoid possible color corrections between the SOFI and 2MASS photometry for more reddened stars. More than 24,000 sources were identified, the vast majority of which were detected in both the H and K bands. We estimate our completeness limits to be about 17th magnitude at H and K and 18th magnitude at J.

3.1. Extinction Map

We used the NICE method (Lada et al. 1994, Alves et al. 1998) to derive extinctions to approximately 24,000 individual stars detected in our deep infrared survey of Globule 2 and to construct a detailed, high resolution map of the distribution of extinction across the cloud. Briefly, we determine the color excess, $E(H-K)$, for each star:

$$E(H-K) = (H-K)_{obs} - (H-K)_{intrinsic} \quad (1)$$

where $(H-K)_{obs}$ is the observed color of the star and $(H-K)_{intrinsic}$ is the intrinsic color of the star. The intrinsic $(H-K)$ color for each star was assumed to be the same as the average color of stars in a nearby, unreddened control field. Using data from the 2MASS

[1]IRAF is distributed by the National Optical Astronomy Observatory, which is operated by AURA under contract to the NSF.

survey we derived $(H-K)_{intrinsic}$ to be 0.201 ± 0.004 magnitudes. Following convention we scaled the color excesses to equivalent visual extinctions, A_Vs, using a standard reddening law, i.e., $A_V = 15.9\ E(H-K)$.

In Figure 2 we present the extinction map for Globule 2 that we derived from our observations by spatially convolving our data with a 15 arc sec gaussian function and sampling at the Nyquist frequency. Figure 2 represents the most detailed map of the globule's extinction yet obtained. It is a significant improvement over the star count map of Racca et al. (1999) primarily because the NICE method produces a direct measurement of the extinctions to individual stars in each pixel rather than a simple count of the numbers of stars. This produces both a more precise and accurate measurement of extinction in each pixel and enables higher angular resolution to be achieved because the uncertainties are less sensitive to counting statistics. Moreover, our deep survey detected about four times as many stars as in the Racca et al. map. The studies of Jones et al. 1980 and Jones et al. (1984) also used measurements of infrared color excess ($E(H-K)$) to individual stars derive the distribution of extinction toward this globule, but they were able to obtain measurements to only about 100 stars behind the globule, more than two orders of magnitude fewer stars than observed in this survey.

Our map shows the globule to exhibit considerable structure, the most prominent feature being a well defined ring at the center of the globule. A hint of the ring structure is also evident in the lower resolution star count maps of Racca et al. The equivalent visual extinction, A_V, produced by the globule ranges from about 3.5 magnitudes in the outer regions to approximately 12 magnitudes in the ring. The map also shows the presence of whispy or filamentary-like structure outside the high A_V ring. At this level of spatial resolution, the cloud does not appear to be as smooth as the B68 cloud which was mapped at similarly high sensitivity and angular resolution (Alves et al. 2001, 2004).

By spatially integrating the extinction map over the area of the globule we derive the total mass of the globule to be 15.1 ± 0.2 $M_\odot$ for the assumed distance of 150 pc which reasonably agrees with the earlier estimates (11 $M_\odot$) of Jones et al. (1980). The quoted uncertainty is primarily due to the uncertainty in the intrinsic colors of the background stars. If we correct for the foreground/background extinction of the more diffuse Coalsack complex ($A_V \approx 3.5$ mag) we estimate a lower mass for the globule of 6.1 ± 0.5 $M_\odot$, where the uncertainty is entirely systematic and dominated by the uncertainty in the foreground/background extinction. The Jean's mass of the cloud can be derived from its temperature and mean density, that is, $M_J = 1.7\ T^{\frac{3}{2}}\ \bar{n}^{-\frac{1}{2}}\ M_\odot$. For $T = 10$ K and $\bar{n} = 2.7 \times 10^3$ cm^{-3} we find $M_J = 10.4$ $M_\odot$. The globule's mass is less than a Jean's mass, suggesting that the globule is globally stable against collapse.

3.2. Radial Density Distribution

Figure 3 displays the radial profile of extinction that we derived for G2. This profile was constructed by azimuthally averaging extinction measurments for stars within circular annuli, 20 arc seconds wide, sampled at the Nyquist frequency and centered at the extinction minimum near the geometric center of symmetry for the map (i.e., $\alpha = 12^h\ 31^m\ 38.6^s$ and $\delta =$ -63^o 43' 42.5"). The radial profile of extinction displays a clear peak of $A_v \sim 11.5$ magnitudes at a radial distance of 55 arc sec. The off-center peak in the radial density profile corresponds to the ring structure observed in the contour map of figure 2. At large radii the extinction profile smoothly declines until it reachs a plateau at $A_v \sim 3.5$ magnitudes near r $\sim$ 290 arc sec. Noted also by Jones et al. (1984) and Racca et al. (1999), this plateau is likely the result of the fact that G2 is embedded in the Coalsack cloud complex. However, we note that inspection of Figure 2 indicates that the extinction due to the general background of material in the Coalsack is perhaps more patchy than suggested by the constant plateau in Figure 3.

For comparison we plot in Figure 3 the predicted column density profile for a pressure truncated isothermal sphere, the so-called Bonnor-Ebert (BE) sphere. The BE profile was fitted in a least-squares iterative procedure to only those points beyond a radius of 60 arc sec, that is, from the center of the ring outward. In addition a constant plateau of background extinction was included in the BE models to correspond to the observations. The BE density profile is clearly much more centrally concentrated than that of G2. However the shape of G2's density profile at increasing radii just outside the ring is well matched by the BE curve. Even though the density profile of G2 departs from that expected for a BE configuration in its central regions, a more detailed comparison of the two profiles can nonetheless provide some useful insights about the physical nature of the cloud.

A BE sphere is a pressure-truncated isothermal ball of gas within which internal pressure everywhere precisely balances the inward push of self-gravity and external surface pressure. The fluid equation that describes such a self-gravitating, isothermal sphere in hydrostatic equilibrium is the following well known variant of the Lane-Emden equation:

$$\frac{1}{\xi^2}\frac{d}{d\xi}(\xi^2\frac{d\psi}{d\xi}) = e^{-\psi} \tag{2}$$

where ξ is the dimensionless radius:

$$\xi = \mathrm{r}/r_c \tag{3}$$

and r_c, is the characteristic or scale radius,

$$r_c = c_s/(4\pi G\rho_0)^{1/2}, \tag{4}$$

where c_s is the sound speed in the cloud and ρ_0 is the density at the origin. Equation 2 is Possion's equation in dimensionless form where $\psi(\xi)$ is the dimensionless potential and is set by the requirement of hydrostatic equilibrium to be $\psi(\xi)$ = -ln(ρ/ρ_0). The equation can be solved using the boundary conditions that the function ψ and its first derivative are zero at the origin. Equation 2 has an infinite family of solutions that are characterized by a single parameter, the dimensionless radius at outer edge (R) of the sphere:

$$\xi_{max} = \mathrm{R}/r_c. \tag{5}$$

Each solution thus corresponds to a truncation of the infinite isothermal sphere at a different outer radius, R. The external pressure at a given R must then be equal to that which would be produced by the weight of material that otherwise would extend from R to infinity in an infinite isothermal sphere. The shape of the BE density profile for a pressure truncated isothermal cloud therefore depends on the single parameter ξ_{max}. As it turns out, the higher the value of ξ_{max} the more centrally concentrated the cloud is. The stability of such pressure truncated clouds was investigated by Bonnor (1956) and Ebert (1955) who showed that when $\xi_{max} > 6.5$ the clouds are in a state of unstable equilibrium, susceptible to gravitational collapse.

Because G2 is embedded in the more extended Coalsack cloud complex we can only trace the extent of the globule's column density profile to the point where the extinction is about 3.5 magnitudes, the level of the general background extinction in the Coalsack complex. This occurs at an angular radial distance of roughly 290 arc sec. This gives us only a lower limit to the actual radius of the globule. For an angular radius of $\Theta_{max} = 290$ arc sec, $\xi_{max} = 5.8$ from the BE profile fit. This value of ξ_{max} does not represent a particularly high degree of central concentration and is consistent with a relatively stable configuration. For comparison, the measured extinction profiles for the B 68 and B 335 clouds yield values of 6.9 and 12.5 for ξ_{max}, respectively (ALL01, Harvey et al. 2001), indicating higher degrees of central concentration. Apparently the starless B 68 cloud is near the critical state. The high value of ξ_{max} derived for B 335 suggests a very unstable configuration for that object which is consistent with the fact that a well developed protostar has already formed in its center. Of course, the value of ξ_{max} derived here for G2 must be considered a lower limit to the true value of ξ_{max} for the cloud since the background extinction due to the Coalsack complex prevents us from determining the actual outer edge of the globule. However, it

is likely that the true outer radius of the globule is not much larger than estimated here. Consider, for example, that if ξ_{max}=6.5, the predicted surface pressure for the globule would be $P_s/k = 2 \times 10^4$ cm^{-3} K. The external pressure at the cloud surface, P_{ext}, provided by the inter-core gas of the Coalsack cloud can be estimated to be $P_{ext} = \rho v^2$ where ρ is the density of the inter-core gas and v its turbulent velocity. For for an interclump density of 10^2 cm^{-3}, characteristic of CO emitting regions in molecular clouds, and a CO linewidth of 1.2 km s^{-1} which is observed for the ^{12}CO gas in the general complex (Nyman et al 1988), we find $P_{ext}/k = 2 \times 10^4$ cm^{-3} K, which is comparable to the surface pressure of the BE cloud at a dimensionless radius of $\xi_{max} = 6.5$. For larger values of ξ the density and surface pressure will be lower and not in equilibrium with the external pressure. Thus, it appears likely that the cloud does not extend significantly beyond an angular radius of 290 arc sec and consequently is likely to be in a sub- or near- critical state and relatively stable. Indeed, the fact that the mass of the globule is found to be sub-Jeans is also consistent with ξ_{max} being less than 6.5.

Our fit does indicate that the density profile of this cloud between angular radii of approximately 50 - 300 arc sec is the same shape as that of a BE sphere out to a dimensional radius of $\xi = 5.8$. This enables us to scale the physical parameters of the cloud using the above equations for ξ_{max} and assuming a normal gas-to-dust ratio. Specifically,

$$\xi_{max} = 10^{-8} \sqrt{\frac{R A_v}{\kappa(\xi_{max}) T}} \tag{6}$$

where A_v is the extinction through the center of the BE cloud, T is the temperature characterizing the gas, and $\kappa(\xi_{max})$ is the dimensionless column density resulting from the integration of the dimensionless radial density profile through the BE cloud. That is:

$$\kappa(\xi_{max}) = \int_0^1 \frac{\rho(r)}{\rho_0} d(\frac{\xi}{\xi_{max}}) \tag{7}$$

Once the shape of the density profile (ξ_{max}) is fixed, knowledge of any two of the remaining three physical parameters (A_v, R, or T) fixes the third. Thus for $\xi_{max} = 5.8$, ($\kappa(5.8) = 0.91$), $A_v = 9$ magnitudes (set by the BE fit to the data), $\Theta_{max} = 290$ arc sec and a distance of 150 pc, we derive a temperature for the cloud of $T_{BE} = 19$ K. The central density, n_0 of the Bonnor-Ebert model is 1.8×10^4 cm^{-3}. The derived BE temperature is higher than the kinetic temperature of 10 K suggested by CO observations of the Coalsack complex (e.g., Nyman et al 1989). Reducing the distance to the cloud to 100 pc would reduce the BE derived temperature close to 10 K. However, as discussed below, CO observations

also indicate that the velocity field of the globule is characterized by significant non-thermal motions and the derived BE temperature need not be reflective of the kinetic temperature in the gas. Instead, the higher derived temperature may indicate the importance of additional sources of pressure, such as turbulence or magnetic fields, for the internal support of the cloud (e.g., Lai et al. 2003).

In the final analysis however, the fact that the observed extinction profile clearly departs from the BE profile in the central regions suggests that physical parameters derived from the fitted BE profile must be regarded with appropriate caution. However, it is interesting to note here that integrating under the two column density profiles results in a comparable total mass ($\sim$ 6 $M_\odot$) for the cloud. The mass deficit corresponding to the difference between the BE and observed density profiles in the center of the cloud is approximately 0.1 $M_\odot$ or only roughly 1-2 % of the total cloud mass. In other words, a small redistribution of mass to the center of the cloud could result in a configuration with a central density concentration similar to that of a BE sphere or a more typical cloud core. Thus, although this cloud is not strictly a BE configuration, it still may not be very far from a state of overall global equilibrium.

3.3. The $C^{18}O$ Molecular-Line Profile

Figure 4 shows the profile of the $C^{18}O$ 2–1 emission line that we obtained near the center of the globule at the coordinates of $\alpha(2000) = 12^h\ 31^m\ 34^s$ and $\delta(2000)$ = -63^o 44' 51". The line appears to be a blend of two components. A simultaneous fit of two gaussian functions to the observed profile reveals the profile to consist of a relatively bright narrow-line component (NLC) blended with a fainter broad-line component (BLC). Specifically, the derived parameters for the peak line temperatures, LSR center velocities and linewidths for the two components of the profile are: 0.96 K $\pm$ 0.03 K, -5.64 $\pm$ 0.02 km s^{-1}, 0.25 $\pm$ 0.02 km s^{-1} and 0.65 $\pm$ 0.03 K, -5.83 $\pm$ 0.02 km s^{-1} , and 0.55 $\pm$ 0.02 km s^{-1} , respectively. The narrow component is redshifted with respect to the broad component with the relative line-of-sight velocity difference being comparable to the sound speed (0.20 km s^{-1}) in a 10 K molecular hydrogen gas. The observed linewidths of the CO emission features in G2 are somewhat smaller than those ($\sim$ 0.7 km s^{-1}) which often characterize globules and cloud cores (e.g., Tachihara, et al. 2002). On the other hand, the G2 linewidths are not as narrow as those in the B 68 cloud whose $C^{18}O$ emission is characterized by a single, thermally broadened component (Lada et al. 2003).

The blended, dual component nature of the molecular emission line profile was not evident or reported in previous ^{12}CO (Nyman, Bronfman, & Thaddeus 1989), $C^{18}O$ (Kato

et al. 1999), NH_3 emission (Bourke et al. 1995) or H_2CO absorption (Brooks, Sinclair & Manefield, 1976) observations of this source. However, most of these earlier observations were made with considerably lower angular resolution than that (24 arc sec) which characterizes our observation. For example, strong H_2CO absorption obtained with an angular resolution of 4.4 arc min by Brooks et al (1976) appears consistent with a single line characterized by a linewidth (corrected for instrumental broadening) of 0.6 $\mathrm{km\,s^{-1}}$ and a line center velocity of V_{lsr} = -5.8 $\mathrm{km\,s^{-1}}$, which is close to the parameters of the BLC of our $C^{18}O$ profile. Since the beamwidth of the H_2CO observations is a factor of ten larger than that of our 2-1 $C^{18}O$ observations, the lack of evidence for a second, narrow component in the H_2CO line profile suggests that the narrow component present in our $C^{18}O$ spectrum is not as spatially extended as the broad component.

Both components are broader than would be expected (0.12 $\mathrm{km\,s^{-1}}$) for $C^{18}O$ molecules in a gas characterized by a temperature of 10 K, indicating a significant non-thermal component to the linewidth. The non-thermal component of the linewidth can be characterized by a temperature, that is $T_{NT} = (\Delta V_{NT})^2 \mu/(8ln2)k$, where μ is the mean molecular mass (2.34 m_H) and ΔV_{NT} is the non-thermal component of the linewidth. These "non-thermal" temperatures are found to be 14 K and 2 K for the broad and narrow components respectively. In the situation where the total pressure in the cloud is a combination of thermal and turbulent pressure components, we can write $P_{tot} = nk(T_{eff})$ where $T_{eff} = T_K + T_{NT}$. Considering each line component separately we find T_{eff} = 24 K and 12 K, respectively. The BE temperature of 19 K derived earlier lies between these two values and its value is thus consistent with the notion that the cloud may not be far from a state of quasi-static dynamical equilibrium in which gravity is balanced by thermal plus turbulent pressure (provided that $\Delta V_{NT} \neq \Delta V_{NT}(r)$). The three dimensional non-thermal velocity dispersions for the two different lines are found to be 0.39 and 0.15 $\mathrm{km\,s^{-1}}$ for the broad and narrow component, respectively. The BLC is characterized by supersonic motions while the NLC by subsonic motions. These motions are not large enough to unbind the cloud even in the absence of any external pressure. We estimate the escape velocity from this cloud ($\sqrt{2GM/R}$) to be approximately 0.5 $\mathrm{km\,s^{-1}}$ which is larger than the velocity dispersion of the broad-line gas, while the estimated virial velocity ($\sqrt{GM/R}$) of 0.4 $\mathrm{km\,s^{-1}}$ is comparable to the velocity dispersion of the broad-line gas. Thus the globule is most likely a bound object.

3.4. The Sigma-A_V Relation: Small Scale Structure

Both the extinction map and radial profile derived from the data represent ordered and uniform spatial samplings of the observations which reveal structural information about the

cloud down to the angular scale of the sampling function used to construct them. Structural information on smaller angular scales is present in the data but lost in the construction of the ordered extinction map and radial profile. The data used to produce these maps consists of more than 24,000 precise, individual extinction measurements. These measurements are randomly distributed across the cloud with relatively poor spatial sampling. However they are characterized by exquisitely high, pencil-beam, angular resolution. Various techniques can be exploited to recover information on spatial scales smaller than those used in making the ordered extinction map and radial profile. One technique is to analyze the relation between σ_{A_V}, the dispersion in a square pixel of an extinction map and corresponding mean A_V derived for that pixel. Lada et al. (1994) showed that useful information about the structure of the cloud on angular scales smaller than the pixel size of the map can be ascertained from the σ_{A_V} – A_V relation. In particular, this relation can be used to set interesting constraints on the amplitude of small scale random spatial fluctuations in a cloud (Lada et al. 1999, Alves et al. 2004), provided that any systematic column density gradients are resolved by the observations. The amplitude of such fluctuations may be a useful metric to describe the degree of supersonic turbulence in a cloud (e.g., Padoan et al 1997).

For a completely smooth cloud, the σ-A_V relation is flat with the dispersion in σ-A_V (as well as its mean value) solely determined by the observational uncertainties in the photometry and the adopted intrinsic color of background stars. This dispersion will be larger in the presence of random, angular fluctuations in extinction that are unresolved in a single map pixel. In addition the σ-A_V relation will display a positive slope in the presence of either unresolved, systematic gradients in extinction (Lada et al. 1999) or random, angular fluctuations in extinction whose scale or amplitude is a function of extinction (e.g., Padoan et al 1997). In the case where systematic density gradients are present in the cloud and are unresolved within an individual map pixel, the magnitude of the slope of the σ-A_V relation will depend on both the magnitude of the density gradient and the pixel size used to construct the map (i.e., $\sigma \sim \frac{dA_V}{dr}\Delta r$; Lada et al. 1999). In the case where unresolved random spatial fluctuations are present, the magnitude of the slope will depend on the functional dependence of the amplitude and/or angular scale of fluctuations on column density.

We determined the σ-A_V relation for Coalsack G2 at varying angular resolutions (45, 30, 20 & 10 arc sec) from maps made with square sampling functions and compared the results. We found the σ-A_V relation to have a positive slope, independent of resolution, suggesting the presence of unresolved structure on all three spatial scales. However, the slope was found to be identical for the 45, 30, 20 arc sec pixels with a measured value of 0.06 ± 0.003. This suggests both that the large scale density gradient is resolved (i.e., $\frac{dA_V}{dr}\Delta r << \sigma_{obs}$) and that the bulk of the unresolved spatial structure is random in nature and originates on angular scales smaller than 20 arc sec. At 10 arc sec resolution, the slope of the σ-A_V relation was

found to be slightly but not significantly flatter, 0.05 ± 0.01. However it is possible that the small scale structure is beginning to be resolved at this scale suggesting that random spatial column density fluctuations have a characteristic scale of ∼ 10 arc sec or smaller. Such features appear to be discernible in the spatial map shown earlier in figure 2.

Figure 5 shows the σ_{A_V} – A_V relation for Coalsack G2 derived from our data using 20 arc sec square pixels. As noted above, the distribution of measurements in this diagram appears relatively flat, suggesting that our observations have resolved much of the structure in the cloud. However, the existence of a measurable slope does suggest the presence of additional unresolved structure within our 20 arc sec pixels. For the Coalsack G2 we find a limit on the amplitude of random, small scale (< 20 arc sec) angular fluctuations in the extinction to be $\delta A_V/A_V \leq 17\%$ at an A_V of 15 magnitudes. The only other cloud for which infrared extinction measurements exist with similarly high angular and spatial resolution is B68. For this cloud Alves et al. (2004) find the σ-A_V relation to be essentially flat at 10 arc sec pixel resolution and placed a limit of $\delta A_V/A_V < 5\%$ at an A_V of 30 magnitudes. This suggests that structure of Coalsack G2 is not as spatially smooth as that of the B68 cloud consistent with the impression derived from the spatial maps of both globules as mentioned earlier.

4. Discussion

4.1. The Nature of the Globule

Our infrared extinction mapping shows that the structure of Tapia's Globule 2 in the Coalsack cloud clearly differs in its central regions from other well studied globules and cloud cores. It is not as centrally condensed as B68 (ALL01), B 335 (Harvey et al. 2002) or L 694-2 (Harvey et al. 2003). This property of the globule was evident in the earliest studies of its extinction profile (Jones et al. 1984). Moreover, our observations reveal a deep central depression in the column density profile of the cloud. Rather than being centrally condensed, the regions of highest extinction form a clear ring structure. The ring cannot be the result of a change in dust properties at high extinction, since our JHK color-color diagram shows that the extinction law is independent of extinction to the highest observed extinctions (see also Racca et al. 2002). Thus the ring represents a true enhancement in the dust column density, and likely an enhancement of the total column density since there is no reason to suspect that the gas-to-dust ratio varies in this object. The relation of this column density ring to the physical structure and nature of the globule, however, depends on the geometry of the globule.

4.1.1. Flattened Geometry and Magnetic Fields

One possible interpretation of the observations is that the globule is a flattened, perhaps oblate structure. Flattened clouds are more susceptable to fragmentation than spherical clouds and in special circumstances can form gravitationally unstable rings (e.g., Bastien 1983; Li 2001) which could fragment to form multiple star systems (Li & Nakamura 2002). These rings are not static structures and are found in the non-magnetic case to move inward at the speed of sound (e.g., Bastien 1983) thus yielding a relatively short evolutionary timescale ($\approx 10^5$ yrs) for the central regions of the globule. However, ring formation requires very specialized initial conditions which include a highly flattend initial state, no rotation, a uniform or flat initial surface density gradient and a mass greatly exceeding the Jean's mass (Bastien 1983, Li 2001). These conditions, particularly the last one, would appear to rule out such models for the G2 cloud. Flattened, oblate clouds are also the expected result of the more generalized and gradual evolution and collapse of magnetized clouds (e.g., Mouschovias 1976). In such an instance the cloud will be flattened along the field lines. For the case of Coalsack G2, the observed symmetry of the ring structure would suggest that we are observing the ring very close to a face-on orientation with an inclination close to 90^o. Thus the magnetic field lines would be expected to be mostly aligned along the line-of-sight, out of, or into, the plane of the sky. However, measurements of the infrared polarization of some 38 background stars observed through the globule by Jones, Hyland and Bailey (1984) suggest a relatively ordered field with a significant component of the field lines oriented in the plane of the sky. However, since such polarization measurements are only sensitive to the component of polarization in the plane of the sky, the possibility of a dominant line-of-sight component of the field still exists. Although if it does exist, such a component would require a relatively strong line-of-sight field, given the magnitudes of the measured polarizations ($\sim$ 1-2%) for the plane of the sky component.

Chandrasekhar and Fermi (1953) showed that for a magnetic field aligned primarily in the plane of the sky the field strength, B, is related to the dispersion in measured polarization angles (σ_Θ), the line-of-sight velocity dispersion of the gas (σ_v) and the gas density (ρ) as follows:

$$\mathrm{B} = \frac{\sigma_v}{\sigma_\Theta}\sqrt{4\pi\rho} \tag{8}$$

For the case of Coalsack G2, we find from the observations of Jones et al. (1984) that $\sigma_\Theta =$ 0.66 radians. For a molecular hydrogen density of $\bar{\mathrm{n}} = 3$ x 10^3 cm^{-3} and $\sigma_v = 0.23$ km s^{-1} , we derive B = 13 μ G for the cloud from the Chandrasekhar-Fermi equation above. We can also estimate the total field strength by assuming equipartition of magnetic, gravitational

and kinetic energy in the usual manner:

$$B = \sqrt{\frac{3\pi\rho}{2ln2}}\ \Delta V_{NT} \tag{9}$$

where ΔV_{NT} is the non-thermal component of the observed linewidth. For the parameters of the Coalsack G2 and with $\Delta V_{NT} = .53$ km s^{-1} we find B = 14 μ G. The close correspondence between the two estimates of the field strength supports the notion that the field lies primarily in the plane of the sky. This would seem to argue against a highly flattened configuration for the geometry of Coalsack G2. For the purposes of further discussion we therefore assume that the globule is more spherical than flattened in shape.

4.1.2. Spherical Geometry, A Core in Transition

For a more spherical cloud geometry, the ring could be interpreted as a high density shell. For an isothermal or polytropic equation of state, the high density shell would also be the location of maximum pressure in the cloud. Such a configuration cannot be in equilibrium with pressure balancing self-gravity, as would be the case for the more centrally condensed Bonnor-Ebert sphere. Thus, the shell must be either collapsing or expanding. An expanding shell might be expected in the case where an additional source of internal pressure was present in the center of the cloud. A newly formed star with a stellar wind would do the trick, however all of the stars we detected in the central regions of the globule appear to be reddened background stars, none exhibit near-infrared excess or are mid-infrared IRAS or MSX sources.

In the absence of such an additional source of internal pressure, the shell would be expected to be in a state of inward collapse, since the weight of the cloud beyond the ring would likely confine any outward expansion. The close correspondence of the observed column density profile of the globule with that of a stable Bonnor-Ebert sphere in all but the central regions suggests that self-gravity and pressure could be in balance at the outer edge of the ring. The steep drop in the density profile of the cloud in the inner regions, compared to that expected for a stable Bonnor-Ebert configuration (figure 3), indicates that the central pressure is not sufficiently high to balance the weight of the cloud and suggests that the inner high density ring should collapse inwards. The timescale for such collapse is relatively short. The sound crossing time for the central regions is given by $\tau_a = \mathrm{r}_r/\mathrm{a}$ where a is the speed of sound and r_r the radius of the ring. For $\mathrm{T}_K = 10$ K, $\mathrm{r}_r = 50$ arc sec, and D = 150 pc, $\tau_a = 2$ x 10^5 yrs. The width of the $C^{18}O$ line profile is found to be 0.55 km s^{-1} which is significantly in excess of that (0.12 km s^{-1}) expected for thermal broadening in a

10 K gas. The dynamical time in the central regions is given by $\tau_d = r_r/\sigma_{NT} = 1.5$ x 10^5 yrs, slightly less than the sound crossing time. Here σ_{NT} is the one-dimensional, non-thermal velocity dispersion assuming a 10 K gas. Both these timescales are less than the estimated lifetime (10^6 years) of a starless core (Lee & Myers 1999).

Another possibility is that the globule is in a state of overall oscillation. For clouds that are in a stable equilibrium state there is a natural tendency to oscillate upon being perturbed. For example, Clarke and Pringle (1997) have shown that such oscillations can arise from imbalances in the local heating and cooling rates in cloud cores. Moreover, more recently Matsumoto and Hanawa (2003) have found that the presence of small amounts of rotation can cause initially unstable and collapsing cloud cores to stablize and oscillate. Indeed, transient central ring structures appear in some of the oscillating clouds in their numerical simulations. Molecular-line observations of B68 have also suggested that non-radial surface pulsations are present in that near- critical cloud (Lada et al 2003). If the ring in G2 were the result of such oscillatory behavior, the oscillations would likely move at the acoustic or sound speed and result in time scales for significant structural change in the central regions of the cloud comparable to that derived above for the implosion of the ring. Although the central ring structure in G2 is out of equilibrium with its surroundings, it is not possible from these data and existing theory to determine whether or not the ring is unstable and imploding or oscillating around some temporary equilibrium state. Nonetheless, these considerations do suggest that the globule is quite young and that its presently observed structure is transient.

Although as a whole the globule may be best described by a globally spherical geometry, the central column density ring is probably not a spherically symmetric structure. Models we have constructed to explain the ring as a limb-brightened spherical shell cannot reproduce the relatively high contrast in extinction between the ring and the central depression. This suggests that the ring may be more toroidal than spherical in shape. Nonetheless, the ring would still likely be a transient structure since material within it would not be in pressure equilibrium with gas in the central regions of the cloud. Independent of the exact details of the cloud geometry, it appears that the globule is in a state of transition, perhaps in the process of transforming into a more centrally condensed state, similar to that of typical Bok globules and dense cores that form stars.

4.2. Turbulence and the Origin of the Ring

The observed $C^{18}O$ line toward the center of Coalsack G2 displays a complex profile consisting of two blended components (i.e., the NLC and BLC). The linewidth of each blended

component is super thermal indicating that significant non-thermal motions characterize the velocity field of this cloud. The origin of the non-thermal component of the linewidths in G2 is likely turbulent motions in the cloud. The three-dimensional turbulent velocity dispersion (0.15 $\mathrm{km\,s^{-1}}$) of the NLC is slightly more than a factor of two lower than that (0.39 $\mathrm{km\,s^{-1}}$) of the BLC, indicating a lower degree of turbulent motions. The turbulent motions in the BLC are supersonic at about Mach 2 while the turbulence in the gas emitting the narrow line is subsonic. The NLC also appears to be less extended than the broad component, yet it is 50% brighter.

The narrow-line feature appears to be absent in observations made with lower angular resolution, in particular, it is not present in H_2CO absorption measurements obtained with a beamwidth of 4.4 arc min, an order of magnitude larger than that of our CO observations (Brooks et al. 1976). This suggests that the NLC has been heavily beam diluted in the H_2CO observations and thus arises in a region less than, or on the order of, 1-2 arc min in extent. In this region the supersonic turbulent motions that characterize the bulk of the cloud have been largely dissipated. Since: 1) the inferred scale of the narrow line region is comparable to the size of the high column density ring, and 2) the coordinates of the CO observation correspond to a location centered on the southwest corner of the high extinction ring, we suggest that the NLC originates within the ring. A high resolution ($\sim$ 30 arc sec) map of $C^{18}O$ emission would enable a direct test of this particular hypothesis. If, however, this proposition is correct, then it is possible that the ring is a high density structure that formed by the collision and compression of turbulent gas elements within the globule. This process likely resulted in shock compression of the gas and the consequent dissipation of turbulent energy which produced the subsonic velocity dispersion in the NLC. In this picture, the dissipation of turbulence results in the formation of the ring structure and the production dense gas in the central regions of the globule. Presumably, as more turbulence is dissipated in the cloud, the cloud would adjust to a more centrally concentrated state. This turbulent model for the origin of the ring would also be consistent with the non-spherical geometry of the ring, including the fact that the NLC and BLC differ in velocity, something that would not be expected in spherical symmetry. This interpretation of the motions of the molecular gas provides additional support for the notion that the G2 core is in an early state of evolutionary development.

5. Summary and Concluding Remarks

A number of considerations from the analysis of our observations of Tapia's Globule 2 in the Coalsack suggest that the globule is a bound core in a state very close to overall dynamical

equilibrium. Perhaps the most compelling of these is the finding that the measured gas motions in the globule, derived from the linewidth of $C^{18}O$ emission, indicate that the cloud is gravitationally bound and may even be near virial equilibrium. Moreover, the density gradient of the cloud, beyond the central ring, is consistent with that of a sub-critical BE cloud in which thermal and non-thermal pressure balance self-gravity. This, in turn, is consistent with the fact that the cloud's mass is found to be less than the Jean's mass. In addition the globule's structure is well resolved by our extinction observations and appears to be relatively smooth, though less smooth than B 68, the only other cloud studied in such detail by infrared extinction measurements.

However, the G2 core differs from typical bound cloud cores in some significant ways. The peak extinction ($A_V \approx 12$ mag.) is relatively low for a dense core. Most importantly, the density structure of the central regions of the G2 cloud departs significantly from that of a typical cloud core and from the predictions for a centrally condensed BE configuration in hydrostatic equilibrium. In particular, the observed column density distribution is characterized by a deep central depression bordered by a well-defined ring of high column density and high pressure. The central ring is likely out of equilibrium with the gas in the very center of the cloud and consequently appears to be a transient feature with an evolutionary time scale of order 10^5 years which is less than the expected million year lifetime of a starless core. This would seem to indicate that the central regions of the cloud are in a phase of structural transition and evolving to a new physical configuration. Given that the central column density depression represents a mass deficit between the observed and best-fit BE density profile of only about 1-2% the total cloud mass, it seems plausible to assume that the cloud will evolve to a more relaxed, BE-like, configuration. The gradual dissipation of turbulence in the central regions of the cloud may be driving this transition. Thus, G2 appears to be a cloud core in an early stage of formation.

The Coalsack complex has long been known to be unusual among molecular clouds in its lack of any significant star forming activity (Nyman et al. 1989). Earlier CO observations have shown that it is also unusual in its relative paucity of dense gas (Kato et al. 1999). These facts are clearly not unrelated since surveys of molecular clouds have demonstrated that stars form exclusively in dense gas (e.g., Lada 1992). The Coalsack complex is plausibly a very young molecular complex. The fact that we find the structure of the most opaque globule in the Coalsack cloud to clearly differ from the steep centrally condensed configurations of star forming cores and globules in other clouds, appears consistent with the idea that this core is also quite young. Exactly how early this core is in its development is difficult to determine. However, many starless cores, for example, B68 (ALL01) and L694-2 (Harvey et al 2004), are known to be characterized by a high degree of central concentration, often similar to star forming cores. If such structure is more typical of starless cores then we would suspect

that G2 represents a rare example of an extremely early phase of dense core evolution. Investigation of the detailed structures of a larger sample of starless cores is clearly needed to better quantify this conjecture. However, we note that although starless cores in molecular clouds are relatively common (Lee & Myers 1999), cloud complexes without star formation are extremely rare. Together these factors suggest the extreme youth of the Coalsack complex and indicate that this region constitutes an important laboratory for future studies of the poorly understood processes of cloud and core formation.

We thank Karoline P. Pershell for able assistance with the infrared data reduction. We acknowledge Andi Burkert, Richard Klein, Alyssa Goodman, Frank Shu and Zhi-Yun Li for useful discussions and an anonymous referee for comments which improved the paper. This work was supported by NASA Origins Grants NAG-9520 and NAG-13041 and by a UT Martin Faculty Research Grant.

REFERENCES

Alves, J., Lada, C.J., Lada, E.A., Kenyon, S.J., & Phelps, R. 1998 ApJ, 506, 292.

Alves, J., Lada, C. J., & Lada, E.A. 2001 Nature, 409, 159.

Alves, J., Lada, C. J., Lada, E. A. & Scannapieco, E. 2004 in preparation.

Bastien, P. 1983, A&A, 119, 109.

Benson, P. J., & Myers, P. C., 1989, ApJS, 71, 89.

Bergin, E. A., Alves, J. A., Huard, T. L. & Lada, C. J. 2002, ApJL, 570, 101.

Bonnor, W.B., 1956 MNRAS, 116, 351.

Bok, B.J. 1948 Centennial Symposia, Harvard College Observatory Monographs, No. 7, 53.

Bok, B.J. 1977 PASP, 89, 597.

Bok, B.J., Sim, E.M., & Hawarden, T.G. 1977 Nature, 266, 145.

Bourke, T.L., Hyland, A.R., Robinson, G, James, S.D., & Wright, C.M. 1995, MNRAS, 276, 1067.

Brooks, J.W., Sinclair, M.W. & Manefield, G.A. 1976, MNRAS, 175, 117.

Cambresy, L. 1999, A&A, 345, 965.

Chandrasekhar, S. & Fermi, E. 1953, ApJ, 118, 113.

Clarke, C. J. & Pringle, J.E. 1997, MNRAS, 288, 674.

Ebert, R. 1955, Zeitschrift fur Astrophysik, 36, 222.

Harvey, D.W.A., Wilner, D., Alves, J., Chen, H., Lada, C.J. & Myers, P.C. 2001, ApJ, 563, 903.

Harvey, D.W.A., Wilner, D, Lada, C.J., Myers, P.C. & Alves, J. 2003 ApJ, in press.

Jones, T.J., Hyland, A.R., Robinson, G., Smith, R. & Thomas, J. 1980, ApJ, 242, 132.

Jones, T.J., Hyland, A.R. & Bailey, J. 1984 ApJ, 282, 675.

Kato, S, Mizuno, N. Asayama, S-I., Mizunk, A., Ogawa, H. & Fukui, Y. 1999 PASJ, 51, 883.

Lada, C.J., Lada, E.A., Clemens, D. & Bally, J. 1994 ApJ, 429, 694.

Lada, C.J., Alves, J. & Lada, E.A. 1999 ApJ, 512, 250.

Lada, C.J., Bergin, E.A., Alves, J.F. & Huard, T.L. 2003, ApJ, 586, 286.

Lada, E. A. 1992, ApJL, 393, 25.

Lai, S-P., Velusamy, T., Langer, W.D. & Kuiper, T.B.H. 2003, ApJ, 126, 311.

Lee, C-W. & Myers, P. C. 1999, ApJS, 123, 233.

Li, Z-Y. 2001, ApJ, 526, 806.

Li, Z-Y. & Nakamura, F. 2001, ApJ, 578, 256.

Matsumoto, T., & Hanawa, T. 2003, ApJ,595, 913.

Martin, R. N., & Barrett, A. H. 1978, ApJS, 221, 124.

Mouschovias, T. 1976, ApJ, 206, 753.

Nyman, L.A., Bronfman, L. & Thaddeus, P. 1989 A&A, 216, 185.

Padoan, P., Jones, B.J.T., & Nordlund, A.P. 1997 ApJ, 474, 730.

Racca, G., Gomez, M. & Kenyon, S. 2002, ApJ, 124, 2178.

Tachihara, K., Onishi, T., Mizuno, A. & Fukui, Y. 2002, A&A, 385, 909.

Tapia, S. 1973, in IAU Symp. 52, Interstellar Dust and Related Topics, ed. J.M. Greenberg & H.C. van de Hulst (Dodrecht; Reidel), 43.

Yun, J.L., & Clemens, D.P. 1990, ApJL, 365, 73.

Full resolution figures and text can be downloaded from
http://cfa-www.harvard.edu/∼clada/preprints.html

Fig. 1.— DSS optical image of Globule 2, the most opaque core in the Coalsack complex. The box outlines the region surveyed in the infrared with the NTT.

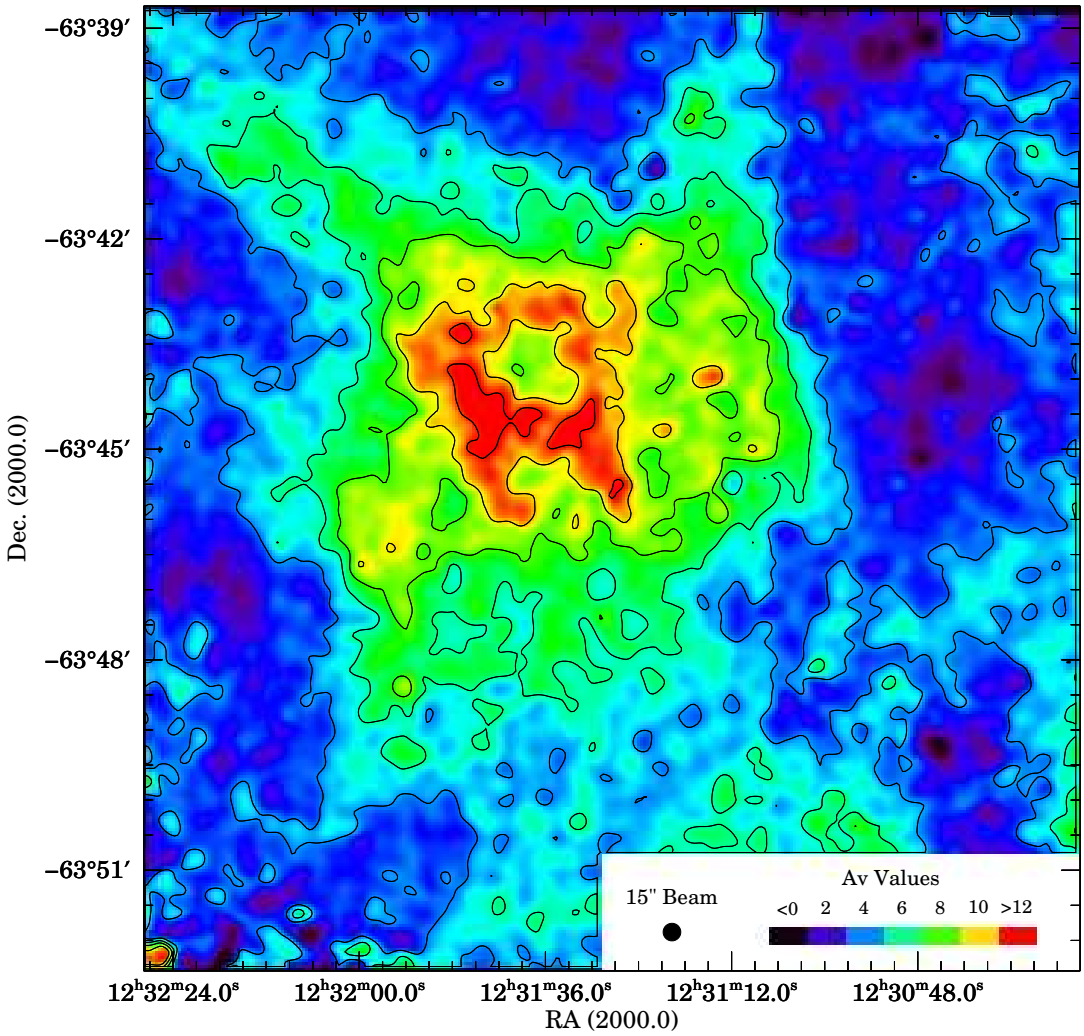

Fig. 2.— Map of the equivalent visual extinction, A_V, in Globule 2 of the Coalsack cloud derived from deep infrared imaging observations. The map was constructed by convolving a 15 arc sec gaussian smoothing function with the pencil-beam extinction measurements of approximately 24,000 stars randomly distributed across the mapped region. A prominent ring of high column density dominates the structure of this cloud. Contours (thin lines) begin at an A_V of 4 magnitudes and increase in steps of 2 magnitudes.

Full resolution figures and text can be downloaded from http://cfa-www.harvard.edu/∼clada/preprints.html

Fig. 3.— Azimuthally averaged radial extinction (column density) profile for Coalsack Globule 2. Also plotted is the expected column density profile of the Bonnor-Ebert sphere that best fits the observations between radii of 55 - 400 arc sec.

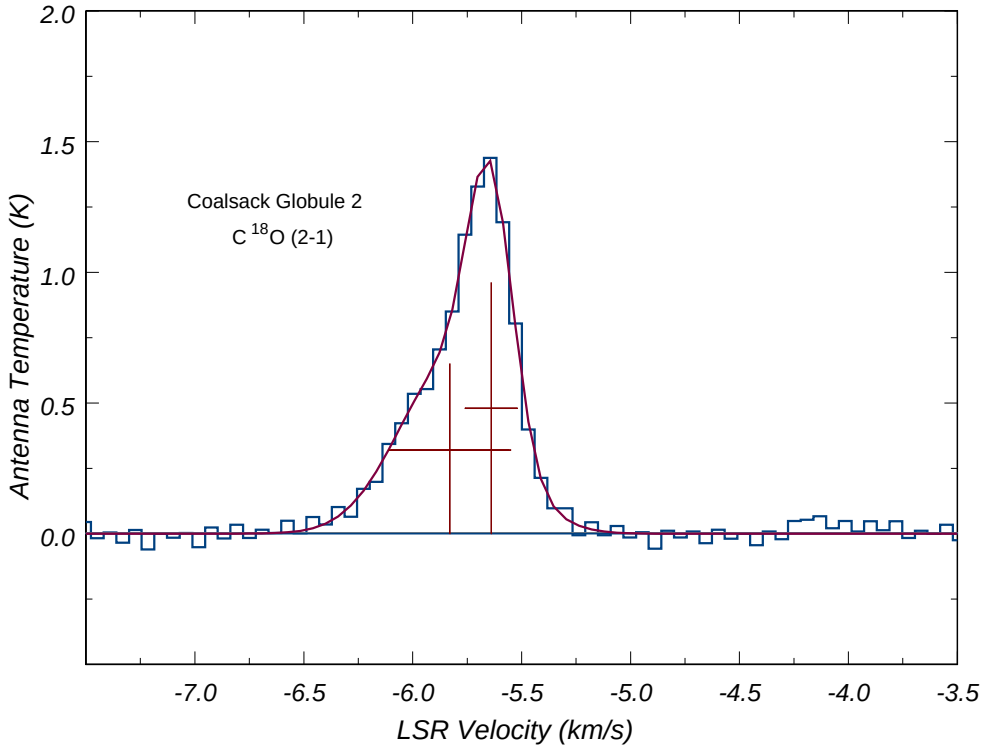

Fig. 4.— The observed line profile of the J = 2 → 1 transition of $C^{18}O$ emission toward the central regions of the globule. The profile consists of a blend of two components whose parameters were derived from a simultaneous fit of two gaussian functions and a linear baseline (smooth line) to the observed spectrum. The crosses mark the locations, amplitudes and linewidths (FWHP) for the two components derived from the gaussian fitting.

Full resolution figures and text can be downloaded from
http://cfa-www.harvard.edu/∼clada/preprints.html

Fig. 5.— The σ - A_V relation for Coalsack Globule 2 derived from measurements obtained with a square spatial sampling function 20 arc sec wide. The relation is relatively flat indicating that the structure in the cloud has been mostly resolved at this resolution and that the cloud is relatively smooth on this angular scale.

This figure "f1.jpg" is available in "jpg" format from:

http://arXiv.org/ps/astro-ph/0404054v1

This figure "f3.jpg" is available in "jpg" format from:

http://arXiv.org/ps/astro-ph/0404054v1

This figure "f5.jpg" is available in "jpg" format from:

http://arXiv.org/ps/astro-ph/0404054v1